

## Video Article

# Imaging the Intracellular Trafficking of APP with Photoactivatable GFP

Joshua H. K. Tam<sup>1</sup>, Stephen H. Pasternak<sup>1,2</sup>

<sup>1</sup>Department of Physiology and Pharmacology, Robarts Research Institute, Western University

<sup>2</sup>Department of Clinical Neurological Sciences, Western University

Correspondence to: Stephen H. Pasternak at [spasternak@robarts.ca](mailto:spasternak@robarts.ca)

URL: <https://www.jove.com/video/53153>

DOI: [doi:10.3791/53153](https://doi.org/10.3791/53153)

Keywords: Cellular Biology, Issue 104, Amyloid precursor protein, Photo-activatable GFP, Golgi, Lysosomes, Intracellular trafficking, Alzheimer's disease,  $\beta$ -amyloid, Live-cell microscopy

Date Published: 10/17/2015

Citation: Tam, J.H., Pasternak, S.H. Imaging the Intracellular Trafficking of APP with Photoactivatable GFP. *J. Vis. Exp.* (104), e53153, doi:10.3791/53153 (2015).

## Abstract

Beta-amyloid ( $A\beta$ ) is the major constituent of senile plaques found in the brains of Alzheimer's disease patients.  $A\beta$  is derived from the sequential cleavage of Amyloid Precursor Protein (APP) by  $\beta$  and  $\gamma$ -secretases. Despite the importance of  $A\beta$  to AD pathology, the subcellular localization of these cleavages is not well established. Work in our laboratory and others implicate the endosomal/lysosomal system in APP processing after internalization from the cell surface. However, the intracellular trafficking of APP is relatively understudied.

While cell-surface proteins are amenable to many labeling techniques, there are no simple methods for following the trafficking of membrane proteins from the Golgi. To this end, we created APP constructs that were tagged with photo-activatable GFP (paGFP) at the C-terminus. After synthesis, paGFP has low basal fluorescence, but it can be stimulated with 413 nm light to produce a strong, stable green fluorescence. By using the Golgi marker Galactosyl transferase coupled to Cyan Fluorescent Protein (GalT-CFP) as a target, we are able to accurately photoactivate APP in the trans-Golgi network. Photo-activated APP-paGFP can then be followed as it traffics to downstream compartments identified with fluorescently tagged compartment marker proteins for the early endosome (Rab5), the late endosome (Rab9) and the lysosome (LAMP1). Furthermore, using inhibitors to APP processing including chloroquine or the  $\gamma$ -secretase inhibitor L685, 458, we are able to perform pulse-chase experiments to examine the processing of APP in single cells.

We find that a large fraction of APP moves rapidly to the lysosome without appearing at the cell surface, and is then cleared from the lysosome by secretase-like cleavages. This technique demonstrates the utility of paGFP for following the trafficking and processing of intracellular proteins from the Golgi to downstream compartments.

## Video Link

The video component of this article can be found at <https://www.jove.com/video/53153/>

## Introduction

The hallmark of Alzheimer's disease (AD) is the presence of senile plaques and neurofibrillary tangles (NFTs) in the brain. The major constituent of senile plaques is  $\beta$ -amyloid ( $A\beta$ ).  $A\beta$  is derived from its precursor, amyloid precursor protein (APP)<sup>1</sup>. The amyloidogenic cleavage of APP begins with removal of the ectodomain from APP by  $\beta$ -secretase<sup>2</sup>. The remaining 99-residue carboxyl terminal fragment (CTF) can be cleaved by  $\gamma$ -secretase to produce  $A\beta$ <sup>3-7</sup>. While many experiments have documented the cleavage of cell surface APP after internalization from the cell surface into the endosomal/lysosomal system, a number of recent studies have suggested that intracellular trafficking of APP is also important in regulating its processing<sup>8-11</sup>.

There have been a number of attempts at modulating the levels of  $A\beta$  with  $\gamma$ -secretase inhibitors and  $A\beta$  immunotherapies. However, recent clinical trials with these therapies showed no benefit, and, in some cases, caused harm<sup>12</sup>. An unexploited strategy to modulate  $A\beta$  production is to alter the sub-cellular localization of APP and  $\gamma$ -secretase interaction. The Golgi, plasma membrane, and endosomes/lysosomes have all been suggested as possible locales for  $\gamma$ -cleavage of APP. Research from our laboratory suggests that APP and the  $\gamma$ -secretase are resident proteins of the lysosomal membrane<sup>13</sup>. Furthermore, we have found that the lysosomal  $\gamma$ -secretase has an acidic optimal pH<sup>13</sup>. In addition, alkalization of the endosomal/lysosomal system with chloroquine or  $NH_4Cl$ , has been shown to decrease the production of  $A\beta$ <sup>14</sup>.  $\gamma$ -secretase inhibition or knockout or Presenilin leads to APP-CTFs accumulation in the lysosome<sup>15-17</sup>. Moreover, disrupting APP endocytosis lowers  $A\beta$  production<sup>18-20</sup>.

Despite the importance of the Golgi as a sorting station for nascent proteins and proteins recycled from the endosomal/lysosomal system, the intracellular trafficking of APP has not been studied in detail<sup>21</sup>. Recent work has shown that APP can be recycled to the trans-Golgi network (TGN) via interaction with the retromer complex. Down regulation of the retromer complex decreases  $A\beta$  production<sup>8,22-24</sup>. However, the egress of APP from the Golgi has not been well studied.

While following the endocytosis of cell-surface proteins, such as the transferrin receptor, are easily labeled and followed, following the trafficking of intracellular proteins is more challenging. In fact, few proteins have had their intracellular trafficking imaged. The advent of fluorescent protein

tags, such as photo-activatable-GFP (paGFP), has provided new tools to examine intracellular trafficking. Photo-activatable-GFP is a form of GFP that is nearly invisible after synthesis, but develops strong green (GFP) fluorescence after being activated by 413 nm laser light and this signal is stable for days<sup>25,26</sup>. Constructs using paGFP have been used to demonstrate the intralysosomal trafficking of the Lysosomal Protein membrane protein 1 (LAMP1)<sup>25</sup>, the cell surface delivery of the Vesicular Stomatitis Virus Glycoprotein (VSVG, a marker of the secretory pathway)<sup>27</sup>, and the turnover of peroxisomes<sup>28</sup> and autophagosomes<sup>29</sup>.

In order to visualize the sorting of APP from the TGN in live cells, we designed plasmid expressing the last 112 amino acids of APP coupled to photo-activatable (paGFP) on the C-terminal (referred to as  $\beta$ APP-paGFP)<sup>30</sup>. We have also performed these experiments with full length APP and achieved similar results; the BAPP construct is used here because it provides brighter images. We then photo-activate  $\beta$ APP-paGFP only in the TGN, as demarcated by the TGN marker Galactosyltransferase (GalT). Although APP has been tagged with paGFP to visualize rapid axonal transport of APP and clearance from the perinuclear region, this is the first demonstration of APP trafficking from one carefully defined compartment to another<sup>11,31,32</sup>. Here, we demonstrate accurate photo-activation within the TGN and the egress of APP into downstream compartments and subsequent cleavage and clearance from lysosomes<sup>30</sup>. The accurate photo-activation within the Golgi is widely applicable to other protein systems.

## Protocol

### 1. Cell Plating and Transfection

1. In a cell culture hood, plate ~300,000 to ~500,000 SN56 cells (a kind gift of Dr. Jane Rylett) on a 35 mm glass-bottom confocal dish and cover with pre-transfection media (Dulbecco's Modified Eagle Medium, DMEM, supplemented with 10% FBS).
2. Incubate cells overnight at 37 °C in a 5% CO<sub>2</sub> incubator to proliferate.  
Note: Cells should be approximately 50%-70% confluent before transfection.
3. In a cell culture hood, transfect cells with plasmids expressing a fluorescent protein tagged TGN marker (Galactosyl transferase coupled to Cyan Fluorescent Protein, GalT-CFP), a fluorescent protein tagged compartment marker (here, lysosome associated membrane protein 1, LAMP1, tagged with mRFP), and the protein of interest tagged with paGFP ( $\beta$ APP-paGFP). (These constructs have previously been described<sup>30</sup>)
4. Incubate cells with transfection reagent and plasmid DNA for 24 hr at 37 °C in a 5% CO<sub>2</sub> incubator. Use a ratio of ~2  $\mu$ g of DNA to 5  $\mu$ l of transfection agent (e.g. Lipofectamine 2000) to best balance cytotoxicity and transfection efficiency. Actual concentrations may need to be optimized for different plasmids. In the experiments described here, use 1  $\mu$ g/confocal dish of  $\beta$ APP-paGFP, 0.3  $\mu$ g/confocal dish of LAMP1-mRFP, and 0.2  $\mu$ g/confocal dish of GalT-CFP.  
Note: The amount of plasmid used will depend on transfection efficiency.
5. For neuronal cell lines: After step 1.4, in a cell culture hood, remove pre-transfection media and differentiate SN56 cells in 2 ml DMEM supplemented with 0.1% penicillin/streptomycin with 1 mM dibutyryl cyclic AMP (dbcAMP) for 24 hr.

### 2. Microscope Stage Preparation

1. Pre-warm phosphate-buffered saline (PBS) and Hank's Balanced Salt Solution (HBSS) to 37 °C. Warm-up microscope stage before imaging to 37 °C.
2. Wash cells twice with PBS, to remove differentiation media and replace with 2 ml of HBSS at 37 °C. Place cells on microscope stage warmed to 37 °C.  
Note: Cells are viable for approximately 1.5-2 hr in HBSS.
3. Allow 5-10 min for the confocal plate temperature to equilibrate with the microscope stage.

### 3. Photo-activation of ROIs over the Golgi

1. With the microscope eyepiece, find cells transfected with GalT-CFP, LAMP1-mRFP, and  $\beta$ APP-paGFP.
  1. Use an oil-immersion lens with high magnification (i.e. 63X or 100X). For visual conformation of fluorescence, use a filter set capable of visualizing FITC (for CFP and GFP fluorescence) and rhodamine (for mRFP fluorescence).
2. Set the confocal slice for each channel to 1  $\mu$ m. Take a low-resolution image.
3. Crop to image only the cell of interest.
4. Using the adjustment knob, manually set the focal plane to the middle of the cell. This is typically the part of the cell where the nucleus is the largest.
5. Draw 3-5 circular Regions of Interests (ROIs) within the TGN (GalT-CFP fluorescence).
  1. To draw ROIs (i.e. in the Zeiss LSM program), select the 'Edit ROI' button in the command console.
  2. Select the circular ROI button.
  3. Click and drag over GalT-CFP positive regions of the cell.  
Note: The photo-bleaching packages for many microscopes have this capability.
6. Take an image of the cell with the overlaid ROIs. Save a copy of the ROIs for later reference.
  1. To save the ROIs to the image, select the 'Macro' button.
  2. Press the 'Load' button to start the 'CopyRoisToOverlay' (file path: c:/AIM/Macros/AdvancedTimeSeries/Utility.lvb).  
Note: A confocal microscope equipped with 475-525 nm (CFP) band pass (BP), a 500-530 nm BP (GFP), and a 560 nm long pass (LP) filter sets are required. An argon laser for 458 nm and 488 nm emission and a HeNe laser for 540 nm emission is also required.
7. Set-up the microscope for a bleach time course.
  1. Set the laser diode (25 mW 405 nm laser) to maximum power.

Caution: Excessive photo-activation could lead to photo-toxicity or damage to cellular membranes. Use eye protection to avoid retinal damage.

2. Set-up the microscope for 120 cycles of imaging.

Note: One imaging cycle consists of bleaching within the ROIs and imaging of the entire cell. This is a bleach time course.

3. Set the microscope to bleach (photo-activate) only the ROIs for 20-30 iterations after every image. The time to image and bleach an image will vary. Set a time delay between images so each cycle is approximately 30 sec.

Note: The imaging portion of each cycle takes approximately 15-30 sec depending on image size. The bleaching for each ROI is about 50 msec. Bleaching of all 4 ROIs for 20 iterations will take 4 sec at the end of each bleach/image cycle.

8. Start the bleach time course.
9. Turn off the bleaching after 15 min (30 cycles of imaging and bleaching), but continue capturing images of the cell.  
Note: Time 0 to 15 min is the 'pulse' period.
10. Continue capturing images for 45 min (without bleaching), to follow the clearance of  $\beta$ APP-paGFP.  
Note: Time 15 to 45 min is the 'chase' period.
11. Using the analysis method described in step 6, co-localize the protein of interest (here,  $\beta$ APP-paGFP) with the compartment of interest (here, LAMP1-mRFP) by making surfaces to each channel.

## 4. Determine the Downstream Compartment

1. To determine if lysosomes (in these experiments) are the final compartment, add membrane-permeable protease inhibitors to cause proteins to accumulate in the lysosome.
  1. For  $\beta$ APP, use 0.5  $\mu$ M L685, 458 (specific  $\gamma$ -secretase inhibitor) overnight or 100  $\mu$ M chloroquine (deacidifies lysosomes) for 30 min before imaging.
2. Find cells and photoactivate as in step 3.1 – 3.8.
3. Image the cell for an additional 45-min (without photo-activation) to determine where  $\beta$ APP-paGFP accumulates in absence of cleavage.
4. Analyze the delivery of protein to lysosomes (or other downstream compartment) and subsequent clearance according to the method described in step 6.

## 5. Ensure Accuracy of Photo-activation within the Golgi

1. Warm-up HBSS to 37 °C.
2. Prepare a 2 ml solution, for every confocal plate to be imaged, of 66  $\mu$ M nocodazole (treatment) or DMSO (control) in HBSS.
  1. For one confocal plate, pipette 2 ml of 37 °C HBSS and add 7.96  $\mu$ l of nocodazole from a 16.60 mM nocodazole stock.
  2. As a control solution, pipette 2 ml of 37 °C HBSS into a 2 ml tube and add 7.96  $\mu$ l of DMSO.
3. Incubate cells in HBSS with nocodazole or DMSO for 5 min before imaging.
4. Find cells as in step 3.1.
5. Before photoactivation, prepare the microscope to take a Z-stack after the photo-activation period.
  1. Click on the 'Z Stack' button. Start scanning using Fast XY.
  2. Adjust the focal plane with the microscope adjustment knob to the top of the cell. Press 'Mark First' to set the first position in the stack.
  3. Adjust the focal plane with the microscope adjustment knob to the bottom (closest to the glass) of the cell. Press 'Mark Last' to set the last position in the stack.
  4. In the Z stack panel, press the 'Z sectioning' button. Set the 'Interval' to 1  $\mu$ m.  
Note: For a higher spatial resolution stack a smaller stack interval, but more images will need to be taken lengthening the imaging period for the stack.
6. Bleach the cells, as described in step 3.7-3.8. Photo-activate and image from 0 min to 15 min (30 frames).
7. Stop imaging after 30 frames. Immediately save an image of the video.  
Caution: Some microscopes may overwrite first video if it is not saved before starting a second imaging sequence.
8. After saving the video, immediately acquire a Z-stack, using the parameters from step 5.5.
9. Co-localize  $\beta$ APP-paGFP with GalT-CFP (or other Golgi marker), as described in step 6.  
Note: CFP photobleaches rapidly and may not be visible by the end of the imaging period. Colocalization may not be possible with GalT-CFP. If colocalization is required, use mRFP to tag GalT.

## 6. Vesicle Filtering and Colocalization

1. Use an analysis program (e.g. Imaris) to make surfaces of the compartment (e.g. LAMP1-mRFP) and a protein of interest (e.g.  $\beta$ APP-paGFP).
2. Enter the 'Surpass' section of the analysis program by clicking on the Surpass button on the top menu bar.
3. Select the Surface wizard button at the top of the left most panel (5<sup>th</sup> button from the left).
4. Select a channel to filter vesicles (i.e.  $\beta$ APP-paGFP fluorescence, protein of interest).
5. Perform background subtraction by submitting the diameter of the largest vesicle in the field to the wizard and press next. The analysis program automatically selects — based on a threshold derived from the largest vesicle in the field — an area in the channel of interest.
  1. Manually adjust the threshold background to refine the selection if needed.
6. At the bottom of the Threshold selection screen, check the 'Split touching objects' option to separate the combined Surfaces.  
Note: If many vesicles are closely grouped together, the analysis program will group these objects under one surface.

1. Choose 10-15 representative vesicles and calculate the average vesicle diameter and enter the result into the wizard.
7. Refine the selected seed points by increasing or decreasing the threshold on 'Quality' (intensity of the channel in the middle of each spot).  
Note: Surfaces of the channel of interest will be created. Further refinement of the selected surfaces can be performed at this point.  
Threshold vesicles based on the number of pixels in each vesicle.
8. Mask the original channel with this surface. To mask, select the 4th tab from the left in the surface creation wizard (pencil).
9. Select 'Mask All'. A new channel with the vesicles of interest will be created.  
Note: During the mask process, an option to duplicate the original channel is offered. Select this option if the original data needs to be saved.
10. Repeat steps 6.1 through 6.7 for the unfiltered channel (*i.e.* LAMP1 mRFP, compartment).
11. At the top tool bar, select the colocalization tool.
  1. In the top panel, as the histograms of the channels to be colocalized appear, select the recently created masked channels.
  2. Select all of available data. There are dark pixels that are sometimes present after analysis. Do not select these pixels in the histogram, they will skew the results.
  3. In the far right panel, select 'Build Coloc Channel'. This creates a new channel containing only the colocalized pixels. The data will be in the same panel under the 'Channel Statistics' button. The data can be exported as a .CSV file.
  4. Use the 'Percent of Material colocalized' statistic. This option takes into account the intensity of the pixels and size of the object.

## Representative Results

Typical results show  $\beta$ APP leaving the TGN and appears to traffic rapidly to LAMP1 (**Figure 1a and b**). During the photo-activation period, vesicles can be seen departing the Golgi destined for lysosomes (**Figure 1b**). Without inhibitor treatment, paGFP fluorescence will be visible in lysosomes while there is photo-activation in the TGN. After stopping photoactivation, the  $\beta$ APP-paGFP is rapidly cleared from the lysosome (compare **Figure 1a to 1b**). Treatment with nocodazole leads to the accumulation of APP within the GalT-CFP labeled compartments and prevents trafficking to lysosomes (**Figure 1c**).

The Swedish mutation of APP (APP<sup>sw</sup>) increases the rate of  $\beta$ -cleavage by 10-fold<sup>34</sup>. With rapid cleavage of  $\beta$ APP<sup>sw</sup>-paGFP, the paGFP fluorescence appears as a diffuse fluorescence signal in the cytosol. Presumably this is the result of rapid  $\beta$ APP cleavage by  $\gamma$ -secretase liberating the C-terminal paGFP in to the cytoplasm (**Figure 2**). In the presence of  $\gamma$ -secretase inhibitor,  $\beta$ APP accumulates within lysosomes.

After delivery of  $\beta$ APP to the lysosome, the paGFP fluorescence is cleared rapidly. The short residence time could be the result of trafficking from the lysosome to another compartment. Conversely, cleavage of  $\beta$ APP by  $\gamma$ -secretase would be expected to lead to diffusion of paGFP fluorescence from the lysosomal membrane (**Figure 3a**). The diffuse fluorescence is more difficult to detect by confocal microscopy. To determine whether  $\beta$ APP is delivered to another compartment or cleared, SN56 cells were treated with a specific inhibitor against  $\gamma$ -secretase (L685, 458) or an alkalinizing agent (chloroquine). The addition of either L685, 458 or chloroquine resulted in APP accumulation in the lysosome (**Figure 3b and c**).

It is commonly accepted that APP is delivered to the cell-surface before being endocytosed and processed in endosomes and lysosomes<sup>35</sup>. However, in our untreated cells, cell-surface  $\beta$ APP could not be detected by confocal microscopy. Photo-activated  $\beta$ APP may not be concentrated in a specific region of plasma membrane. Instead, there may be a diffuse fluorescence across the large surface area of the plasma membrane. Interestingly,  $\gamma$ -secretase inhibitor treatment leads to detectable  $\beta$ APP-paGFP at the cell surface (**Figure 3b**).  $\gamma$ -secretase inhibitor treatment may route more  $\beta$ APP to the cell surface, in addition to inhibiting enzyme function. Therefore, the large surface area of the plasma membrane spreads paGFP over a larger area and makes detection difficult, although the protein is trafficked to the compartment.

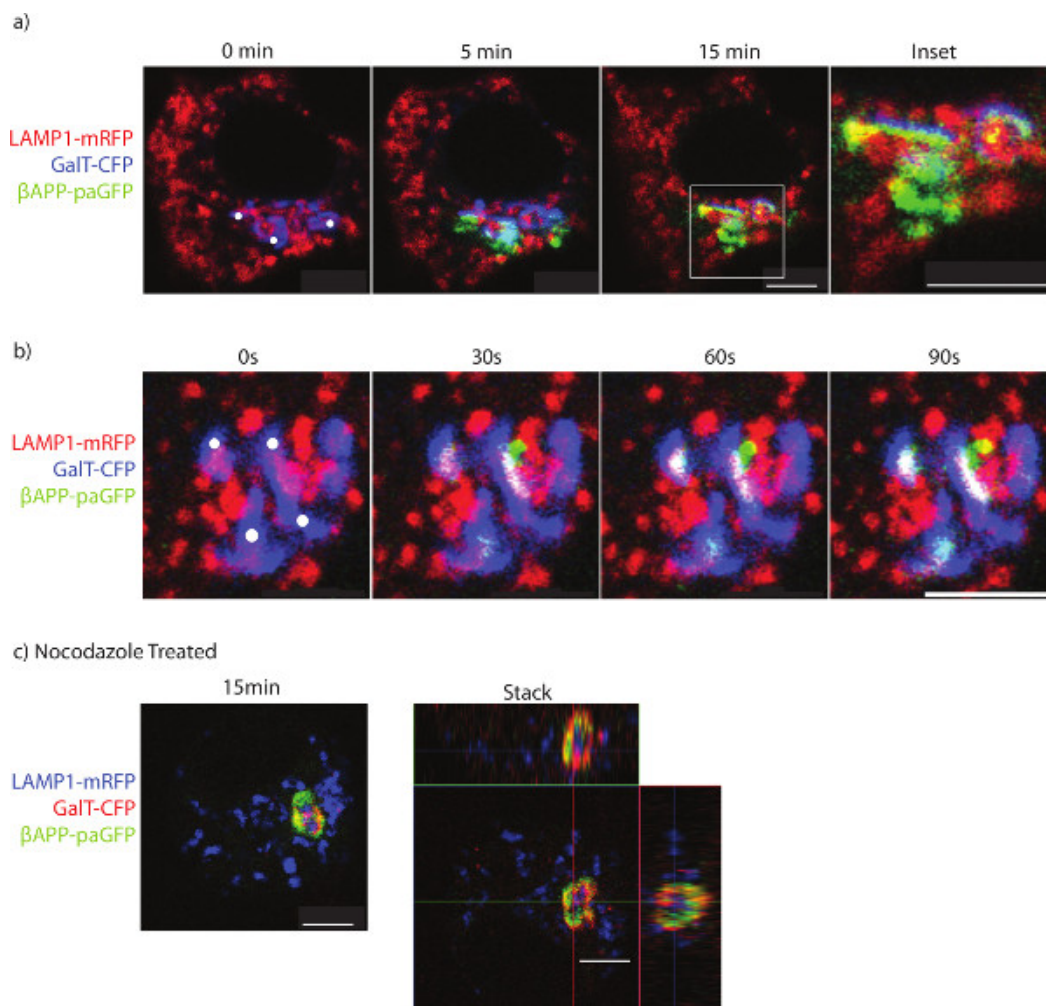


**Figure 1. Imaging the trafficking of APP to lysosomes.** SN56 cells were transfected with LAMP1-mRFP, GalT-CFP, and  $\beta$ APP-paGFP. **a)** The cell was accurately photo-activated within ROIs placed over the Golgi (ROIs denoted by white circles). The cell was alternatively photo-activated and imaged for 15 min to determine  $\beta$ APP-paGFP trafficking. Inset shows trafficking within the perinuclear area from Golgi to lysosomes. Co-localized pixels appear yellow. **b)** The trafficking of a vesicle containing  $\beta$ APP-paGFP to the lysosome. Yellow pixels denote LAMP1 and  $\beta$ APP-paGFP colocalization. **c)** SN56 cells were treated with nocodazole before imaging to prevent  $\beta$ APP-paGFP egress from the TGN. A representative image taken from the end of the photo-activation period. In the right panel, a Z-stack of the same cell taken immediately after photo-activation. The GalT-CFP has been false colored red to improve visualization of colocalized GalT-CFP and  $\beta$ APP-paGFP. Yellow pixels denote colocalization between GalT-CFP and  $\beta$ APP-paGFP. Scale bars represent 5  $\mu$ m. [Please click here to view a larger version of this figure.](#)

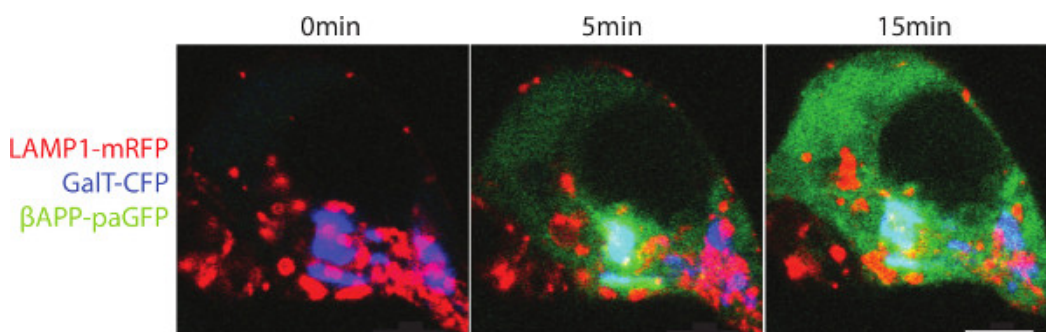


**Figure 2. Trafficking of  $\beta$ APP<sup>sw</sup>-paGFP.** SN56 cells were transfected with LAMP1-mRFP, GalT-Cfp and  $\beta$ APP<sup>sw</sup>-paGFP ( $\beta$ APP with the familial Swedish mutation). The Swedish mutation increases the rate that APP is cleaved. Cells were alternatively within the Golgi photo-activated and imaged. A diffuse fluorescence can be seen after paGFP is detached from the lysosomal membrane to diffuse into the cytoplasm. Scale bar represents 5  $\mu$ m. [Please click here to view a larger version of this figure.](#)

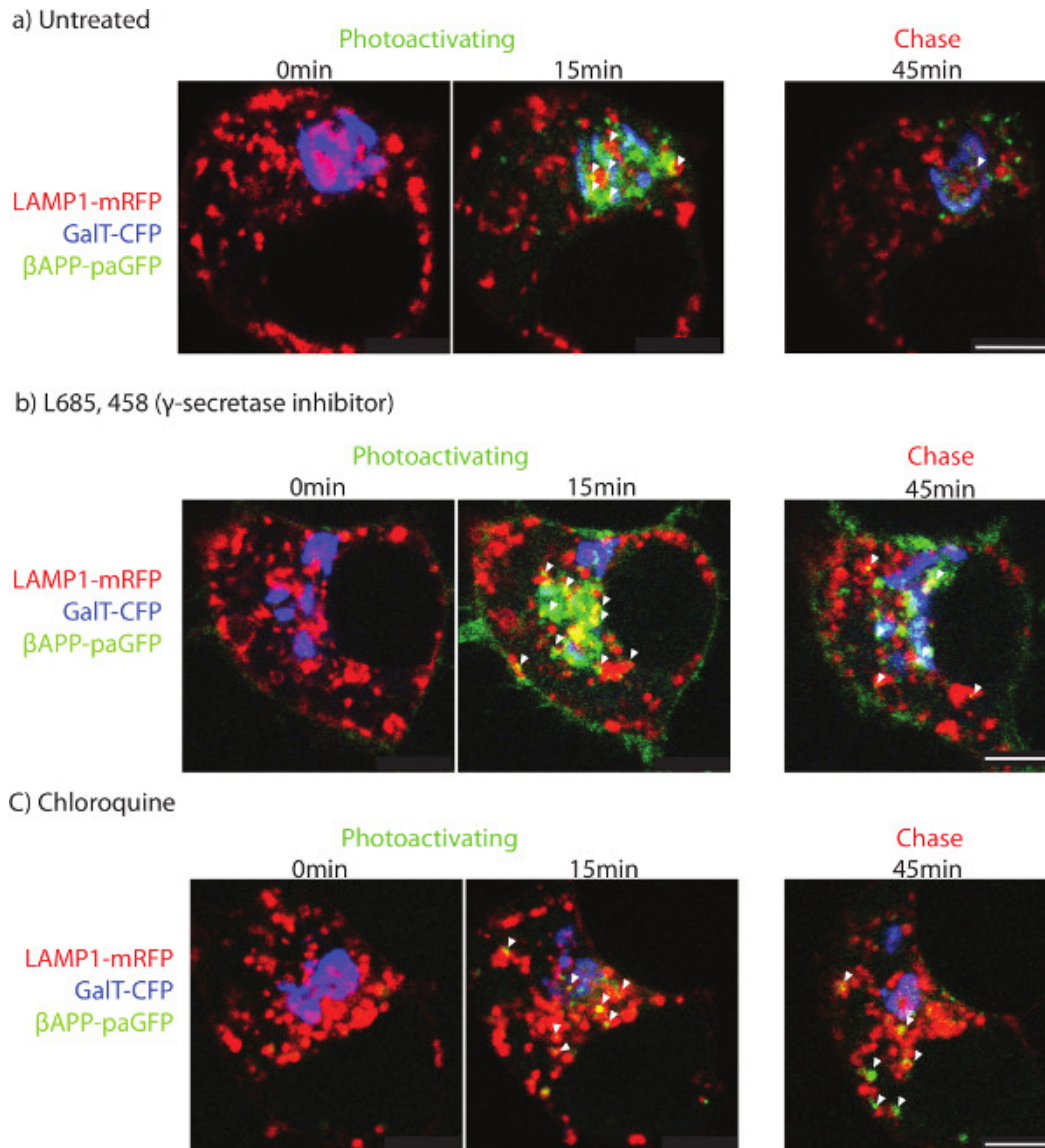


**Figure 3. Determining the terminal organelle.** SN56 cells were transfected with LAMP1-mRFP, GalT-CFP and  $\beta$ APP-paGFP. After photo-activation, cells were followed for an additional 45 min. The two left-most panels show the cells before photoactivation (left-most) and 15 min after photoactivation (middle). The panel on the far right shows APP fluorescence after 45 min of total imaging in **a**) untreated, **b**)  $\gamma$ -secretase inhibitor treated, or **c**) chloroquine treated. Arrowheads point to APP co-localized with LAMP1 after 45 min of imaging. Scale bars represent 5  $\mu$ m. [Please click here to view a larger version of this figure.](#)

## Discussion

This technique describes the accurate photo-activation of membrane proteins tagged with paGFP in the TGN to visualize subsequent trafficking and cleavage. While paGFP was created over a decade ago<sup>25</sup>, this is the first example of accurate photo-activation to follow the trafficking of nascent proteins to downstream compartments. Previous studies using APP-paGFP constructs photo-activated a peri-nuclear region of the cell, which was considered to be the Golgi<sup>11</sup>. However, as evident in our micrographs, lysosomes, early endosomes, and late endosomes can also be found in this region (**Figure 1** and reference 30). These experiments have been run successfully in HEK293 cells, COS7 cells, neuronal SN56 cells, SH-SY5Y cells, and mouse neurons, although the transfection efficiency of mouse neurons is low. Similar experiments have been performed using full length APP constructs and shortened constructs, which include the last 112 amino acids of APP, with the  $\beta$ - and  $\gamma$ -cleavage sites, fused to paGFP. The shortened constructs are easier to transfect and provide a higher fluorescent signal, and these are shown in the accompanying figures. Our shortened constructs also lack the N-terminal ectodomain, which has undefined cleavages and sorting signals<sup>38</sup>. Despite these N-terminal signals and cleavages, we find that our shortened construct has similar localization and trafficking as a full-length APP-paGFP<sup>30, 33</sup>.

Because of the many organelles in the peri-nuclear area of the cell, every effort was made to ensure the accuracy of photo-activation. During the imaging period, the cell and the Golgi will move. Therefore, the photo-activation ROIs must be carefully monitored during the photo-activation

period and adjusted to remain on top of the Golgi. Confocal microscopes are sensitive to small changes in temperatures. For example, AC or heating vents over the microscope could result in a change of the imaging plane.

In order to maintain consistency between experiments, we set a time delay between each photo-activation/imaging cycle. Time is required to bleach the ROIs and image the cell. Depending on the size of the cell and number of ROIs, the time to bleach and take one image will vary. In order to maintain consistency from image to image, set a time delay between images so each image, including bleaching, requires approximately 30 seconds. Increased temporal resolution can be achieved by using detection systems that employ a beam shaper (e.g. LSM5 Live detector). These microscopes can image at 120 frames/second with no loss in resolution.

To confirm the accuracy of photo-activation, it is imperative to perform a nocodazole control. By blocking transport out of the Golgi during photo-activation, this ensures that paGFP is not being significantly activated in the other compartments. CFP photo-bleaches rapidly with repeated imaging and bleaching and can make colocalization with GalT-CFP difficult. If the bulk of paGFP fluorescence stays in the Golgi area, this can also indicate accurate photo-activation. Alternatively, GalT can be tagged with mRFP, which is more photo-stable than CFP in these experiments.

Improved activation within the Golgi can also be achieved with a multi-photon microscope. While the confocal imaging plane in these experiments is typically a 1  $\mu$ m slice, the laser for imaging and photo-activation will pass through the entire cell. A multi-photon laser could be used for these experiments, and may improve accuracy in all three dimensions<sup>35</sup>. However, as demonstrated here, a traditional 405 nm laser diode is sufficient to accurately photo-activate  $\beta$ APP-paGFP within the TGN.

As a control, we have performed similar experiments for VSVG-paGFP fluorescence. VSVG-paGFP, which is constitutively delivered to the cell surface<sup>27,37</sup>, was visualized being delivered to specific subregions of the plasma membrane<sup>30</sup>. This assures that transport to intracellular compartments is not triggered by over-expression or the presence of the paGFP tag.

Diffuse paGFP fluorescence may be difficult to localize by confocal microscopy. In our experience, APP is rapidly cleaved and appears to have a short lifetime as a full-length protein at the lysosomal membrane. This problem is exacerbated by the Swedish FAD mutation that accelerates the rate of APP cleavage<sup>34</sup>. To employ the technique for rapidly cleaved proteins, an inhibitor is crucial to determine the final downstream compartment. Inhibition of  $\gamma$ -secretase by L685, 458 or chloroquine lead to significant accumulation of APP in lysosomes; even with the Swedish mutation.

If too much inhibitor is used, this could lead to intracellular accumulation of  $\beta$ APP-paGFP, and may lead to protein inclusions. Accumulated paGFP in inclusions results in fluorescent paGFP inclusions in the cell before the experiment has started (our unpublished observations, *i.e.* treating overnight with 40  $\mu$ M chloroquine). An inhibitor concentration that prevents cleavage of the protein of interest, but does not lead to inclusion formation should be used. Over-transfection of cells with paGFP can also cause obvious inclusions of paGFP, which will fluoresce without photo-activation. Newly photo-activated paGFP will preferentially traffic to these inclusions and interfere with the interpretation of the results. When looking for cells to image, avoid cells with obvious paGFP inclusions. In our experience with  $\beta$ APP-paGFP, there is a very faint green fluorescence in cells that express  $\beta$ APP-paGFP at the appropriate level. This faint fluorescence typically cannot be imaged and can only be seen through the eyepiece.

Another limitation of this technique is that protein trafficked to a large membrane structure (*i.e.* plasma membrane) may be difficult to detect. This may be because the fluorescent signal, being spread over a large area, is diluted or because the membrane profile in cross section is below the resolution of the confocal microscope. It may be possible to circumvent this problem by imaging using an epifluorescence microscope. However, this will significantly reduce the spatial resolution of the technique.

An advantage of this technique is its applicability to other membrane proteins. While this technique depends on over expression of several proteins, it appears that protein trafficking is not overtly disrupted, as has been demonstrated with VSVG-paGFP and  $\beta$ APP-paGFP<sup>30</sup>. In addition to the lysosome, other markers of the endosomal/lysosomal system have also been used successfully. These include rab5-mRFP for the early endosome and rab9-mChFP (cherry fluorescent protein) for the late endosome. This powerful microscopy technique can be extended to follow the trafficking of other proteins from the TGN. It could equally be applied to follow trafficking between discrete compartments provided well-defined compartment markers are available.

## Disclosures

The authors have no competing financial interests or conflicts of interest.

## Acknowledgements

This work was funded by a grant from the Canadian Institute for Health Research MOP 82890 to SHP. The authors wish to thank G.H. Patterson and J. Lippincott Schwartz for the paGFP construct. SN56 cells were a gift of Dr. Jane Rylett.

## References

1. Masters, C. L., *et al.* Amyloid plaque core protein in Alzheimer disease and Down syndrome. *Proc. Natl. Acad. Sci. U.S.A.* **82** (12), 4245-4249 (1985).
2. Vassar, R., *et al.* Beta-secretase cleavage of Alzheimer's amyloid precursor protein by the transmembrane aspartic protease BACE. *Science*. **286** (5440), 735-741, (1999).
3. De Strooper, B., *et al.* Deficiency of presenilin-1 inhibits the normal cleavage of amyloid precursor protein. *Nature*. **391** (6665), 387-390, (1998).

4. Xia, W., *et al.* Presenilin complexes with the C-terminal fragments of amyloid precursor protein at the sites of amyloid beta-protein generation. *Proc. Natl. Acad. Sci. U.S.A.* **97** (16), 9299-9304, (2000).
5. Li, Y. M., *et al.* Presenilin 1 is linked with gamma-secretase activity in the detergent solubilized state. *Proc. Natl. Acad. Sci. U.S.A.* **97** (11), 6138-6143, (2000).
6. Kim, W., & Hecht, M. H. Sequence determinants of enhanced amyloidogenicity of Alzheimer A $\beta$ 42 peptide relative to A $\beta$ 40. *J. Biol. Chem.* **280** (41), 35069-35076, (2005).
7. Pawar, A. P., *et al.* Prediction of 'aggregation-prone' and 'aggregation-susceptible'. *J. Mol. Biol.* **350** (2), 379-392, (2005).
8. Wen, L., *et al.* VPS35 haploinsufficiency increases Alzheimer's disease neuropathology. *J. Cell Biol.* **195** (5), 765-779, (2011).
9. Rogaeva, E., *et al.* The neuronal sortilin-related receptor SORL1 is genetically associated with Alzheimer disease. *Nat. Genet.* **39** (2), 168-177, (2007).
10. Andersen, O. M., *et al.* Neuronal sorting protein-related receptor sorLA/LR11 regulates processing of the amyloid precursor protein. *Proc. Natl. Acad. Sci. U.S.A.* **102** (38), 13461-13466, (2005).
11. Schmidt, V., *et al.* SorLA/LR11 regulates processing of amyloid precursor protein via interaction with adaptors GGA and PACS-1. *J. Biol. Chem.* **282** (45), 32956-32964, (2007).
12. Moreth, J., Mavoungou, C., & Schindowski, K. Passive anti-amyloid immunotherapy in Alzheimer's disease: What are the most promising targets? *Immun. Ageing.* **10** (1), 18, (2013).
13. Pasternak, S. H., *et al.* Presenilin-1, nicastrin, amyloid precursor protein, and gamma-secretase activity are co-localized in the lysosomal membrane. *J. Biol. Chem.* **278** (29), 26687-26694 (2003).
14. Schrader-Fischer, G., & Paganetti, P. A. Effect of alkalizing agents on the processing of the beta-amyloid precursor protein. *Brain Res.* **716** (1-2), 91-100, (1996).
15. Golde, T., Estus, S., Younkin, L., Selkoe, D., & Younkin, S. Processing of the amyloid protein precursor to potentially amyloidogenic derivatives. *Science.* **255** (5045), 728-730, (1992).
16. Higaki, J., Quon, D., Zhong, Z., & Cordell, B. Inhibition of beta-amyloid formation identifies proteolytic precursors and subcellular site of catabolism. *Neuron.* **14** (3), 651-659, (1995).
17. Chen, F., *et al.* Carboxyl-terminal Fragments of Alzheimer beta -Amyloid Precursor Protein Accumulate in Restricted and Unpredicted Intracellular Compartments in Presenilin 1-deficient Cells. *J. Biol. Chem.* **275** (47), 36794-36802, (2000).
18. Perez, R. G., *et al.* Mutagenesis identifies new signals for beta-amyloid precursor protein endocytosis, turnover, and the generation of secreted fragments, including Abeta42. *J. Biol. Chem.* **274** (27), 18851-18856, (1999).
19. Cirrito, J. R., *et al.* Endocytosis Is Required for Synaptic Activity-Dependent Release of Amyloid- $\beta$  In Vivo. *Neuron.* **58** (1), 42-51, (2008).
20. Carey, R. M., Balcz, B. A., Lopez-Coviella, I., & Slack, B. E. Inhibition of dynamin-dependent endocytosis increases shedding of the amyloid precursor protein ectodomain and reduces generation of amyloid beta protein. *BMC Cell Biol.* **6**, 30, (2005).
21. Traub, L. M., & Kornfeld, S. The trans-Golgi network: a late secretory sorting station. *Curr. Opin. Cell Biol.* **9** (4), 527-533, (1997).
22. Vieira, S. I., *et al.* Retrieval of the Alzheimer's amyloid precursor protein from the endosome to the TGN is S655 phosphorylation state-dependent and retromer-mediated. *Mol. Neurodegener.* **5** (1), 40, (2010).
23. Sullivan, C. P., *et al.* Retromer disruption promotes amyloidogenic APP processing. *Neurobiol. Dis.* **43** (2), 338-45, (2011).
24. Fjorback, A. W., *et al.* Retromer binds the FANSHY sorting motif in SorLA to regulate amyloid precursor protein sorting and processing. *J. Neurosci.* **32** (4), 1467-1480, (2012).
25. Patterson, G. H., & Lippincott-Schwartz, J. A Photoactivatable GFP for Selective Photolabeling of Proteins and Cells. *Science.* **297** (5588), 1873-1877, (2002).
26. Patterson, G. H., & Lippincott-Schwartz, J. Selective photolabeling of proteins using photoactivatable GFP. *Methods.* **32** (4), 445-450, (2004).
27. Hirschberg, K., *et al.* Kinetic analysis of secretory protein traffic and characterization of golgi to plasma membrane transport intermediates in living cells. *J. Cell Biol.* **143** (6), 1485-1503, (1998).
28. Kim, P. K., Mullen, R. T., Schumann, U., & Lippincott-Schwartz, J. The origin and maintenance of mammalian peroxisomes involves a de novo PEX16-dependent pathway from the ER. *J. Cell Biol.* **173** (4), 521-532, (2006).
29. Hailey, D. W., *et al.* Mitochondria supply membranes for autophagosome biogenesis during starvation. *Cell.* **141** (4), 656-667, (2010).
30. Tam, J. H. K., Seah, C., & Pasternak, S. H. The Amyloid Precursor Protein is rapidly transported from the Golgi apparatus to the lysosome and where it is processed into beta-amyloid. *Mol. Brain.* **7** (1), 54, (2014).
31. Scott, D. A., Das, U., Tang, Y., & Roy, S. Mechanistic logic underlying the axonal transport of cytosolic proteins. *Neuron.* **70** (3), 441-454, (2011).
32. Herl, L., *et al.* Mutations in amyloid precursor protein affect its interactions with presenilin/gamma-secretase. *Mol. Cell. Neurosci.* **41** (2), 166-174, (2009).
33. Lorenzen, A., *et al.* Rapid and Direct Transport of Cell Surface APP to the Lysosome defines a novel selective pathway. *Mol. Brain.* **3** (1), 11, (2010).
34. Thinakaran, G., Teplow, D. B., Siman, R., Greenberg, B., & Sisodia, S. S. Metabolism of the 'Swedish' amyloid precursor protein variant in neuro2a (N2a) cells. Evidence that cleavage at the beta-secretase site occurs in the golgi apparatus. *J. Biol. Chem.* **271** (16), 9390-9397, (1996).
35. Thinakaran, G., & Koo, E. H. Amyloid Precursor Protein Trafficking, Processing, and Function. *J. Biol. Chem.* **283** (44), 29615-29619, (2008).
36. Schneider, M., Barozzi, S., Testa, I., Faretta, M., & Diaspro, A. Two-Photon Activation and Excitation Properties of PA-GFP in the 720-920-nm Region. *Biophys. J.* **89** (2), 1346-1352, (2005).
37. Sevier, C. S., Weisz, O. A., Davis, M., & Machamer, C. E. Efficient export of the vesicular stomatitis virus G protein from the endoplasmic reticulum requires a signal in the cytoplasmic tail that includes both tyrosine-based and di-acidic motifs. *Mol. Biol. Cell.* **11** (1), 13-22, (2000).
38. Muresan, V., Varvel, N. H., Lamb, B. T., & Muresan, Z. The cleavage products of amyloid-beta precursor protein are sorted to distinct carrier vesicles that are independently transported within neurites. *J. Neurosci.* **29**, 3565-3578, (2009).